VOCATIONAL TRAINING PROJECT

TOPIC: Comparative Analysis of Predictive Models for Blast Fragmentation

BY

Rahul Kumar Sharma
20JE0749

B.Tech (Mining Engineering)

Department of Mining Engineering
Indian Institute of Technology (Indian School of Mines)
Dhanbad-826004

Under the guidance of **Dr. Ranjit Kumar Paswan**,
Department of Rock Excavation Engineering
CISR-CIMFR
DHNABAD-**826015** (JHARKHAND)

May 2024

TABLE OF CONTENT

ABSTRACT

This paper represents a comparative analysis of predictive model for bench blast fragmentation. A novel Multivariant Regression Analysis (MRA) model is evaluated against established blasting model for comparative analysis. The main focus in this paper will be on the multivariant regression analysis model in predicting the bench blast fragmentation, using separate datasets for model development training and validation.

The Multivariant Regression (MRA) model is compared with well-known and used blasting model, Artificial Neuron Network (ANN) model. Several performance evaluating metrics are used for evaluating the predictive model to assess the accuracy and reliability of the predictive model which includes Mean Absolute Error (MAE), Mean Absolute Percentage Error (MAPE), the Root Mean Square Error (RMSE), and Relative Root Mean Square Error (RRMSE).

The result of the study highlights the effectiveness of the multivariant regression model in predicting bench blast fragmentation in mining scenario. Multivariant regression model incorporate various parameters to predicts the bench blast fragmentation. The parameters includes; No. of Holes, Depth of Holes, Bench Height, Burden, Spacing, Top Stemming, Average Explosive Quantity used per hole, Maximum Explosive Quantity used per hole, Total Explosive Quantity used, and Charge Factor. And the multivariate regression model has lower MAE, MAPE, RMSE and RRMSE value than that of the artificial neuron network (ANN) model, which shows its capability to provide precise and accurate prediction of blast fragmentation.

The research highlights the potential of multivariate regression analysis in improving blast fragmentation prediction for underground mining. By offering more precise predictions, this model can help optimize blasting operations, leading to enhanced productivity and operational efficiency in mines.

CHAPTER-1
INTRODUCTION

Blast fragmentation is a critical factor and plays a pivotal role in mining operations, which influences the productivity, safety, operation cost, and overall efficiency of the mining operations. Accurate prediction of blast fragmentation size distribution is essential for optimizing various mining processes. The mining industry, along with various processing and building industries, places significant emphasis on the process of fragmentation, which involves breaking down material into smaller pieces. This process is crucial for enhancing the efficiency of subsequent operation. The effectiveness of downstream processes is heavily influenced by the characteristics of the initial rock fragments produced by blasting.

Experts like Roy et al. and Mackenzie are shedding lights on the significant role of blasting in both mining as well as in construction industries Their research shows how rock fragmentation adversely affects the operations like loading, hauling, crushing rate, grinding capability, and ore recovery in mining and processing plants. Effective fragmentation impacts not just the immediate task of breaking down rocks but also extends to downstream processes like crushing and grinding. This, in turn, affects the efficiency of the entire mine-to-mill operation and the final product size distribution. Essentially, the quality of fragmentation can set off a chain reaction of improvements or challenges throughout the entire production process. Implementing optimized blasting techniques and refining the processes used to break down materials in mining can greatly boost productivity and improve overall plant performance. However, Studies show that these improvements not only make the processes more efficient but also enhance crusher performance, reduce maintenance, and repair costs, and save money on drilling and blasting. Effective blasting impacts everything downstream, from crushing to grinding, affecting the entire operation from the mine to the mill and the final product size. This ripple effect highlights the importance of precision in blasting. Mastering this technique can lead to greater efficiency, cost savings, and a fundamental improvement in mining operations.

Predicting rock fragmentation is crucial for optimizing rock blasting, which in turn boosts productivity, reduces operational costs, and improves resource utilization. It also lowers energy consumption in downstream processes and enhances production, thereby increasing the profitability of mining operations. To effectively understand and manage the blasting process and its costs, it's essential to predict and evaluate the resulting rock size distribution.

This highlights the need to be consider fragmentation models in blasting. Changing the blasting parameters alters the resulting particle size distribution, which impacts all the downstream processes. Accurately predicting the fragmentation size distribution before blasting is crucial for ensuring desired output. Over the year, many blast fragmentation models have been developed. Some of the most common and widely used include the Rosin-Rammler Distribution, the Swebrec fragmentation curve, the Kuz-Ram fragmentation model, the Kuznetsov-Cunnungham-Ouchterlony (KCO) fragmentation model, and Artificial Neuron

Network (ANN). These models were designed mainly for surface blasting, not for underground blasting. Each model has its own advantage and disadvantages, which makes finding the best fit for a given situation more complex. Basically, Rock the fragmentation depends on the two types of parameter; Controllable parameters and Uncontrollable parameter. Controllable parameters are those parameters which we can change according to our need or desired result of fragmentation. And Uncontrollable parameter are the inherent characteristic of the rockmass.

Multivariate regression analysis presents a promising approach to predict blast fragmentation outcomes in underground applications by considering multiple influencing factors simultaneously. By incorporating variables such as burden, spacing, detonation velocity, hole diameter, blast sequencing, and rock strength, multivariate regression models aim to provide more accurate and adaptable predictions tailored to specific blasting conditions. The availability of fragmentation models to optimize the mining and milling process is fundamental given that when using such models, it is possible to establish what parameters or variables need the most special attention or consideration to produce the desired fragmentation results. Given the constantly changing conditions in mining, such as geology, stress conditions, and mining procedures, any model used in this field must be flexible, adaptable, and dynamic to provide predictions in an acceptable range of accuracy.

This paper aims to contribute to the ongoing discussion about blast fragmentation prediction by comparing a new multivariate regression analysis model with existing predictive models. Specifically, it will compare the performance of the multivariate regression model with the Artificial Neuron Network (ANN) in estimating underground blast fragmentation. By thoroughly examining and comparing these models, the paper seeks to identify their strengths, weaknesses, and areas for improvement. The ultimate goal is to provide valuable insights into the effectiveness of different models in predicting underground blast fragmentation, enhancing understanding in the field, and informing practical applications.

CHAPTER-2
LITRATURE REVIEW

The size distribution of fragments in a muckpile is crucial for the efficiency of downstream operations like loading, transporting, and crushing (Aler et al., 1996). A muckpile contains fragments of various sizes, and any fragment too large to be loaded by an excavator's bucket is considered oversized. Oversized fragments produced during blasting need secondary breakage, either through additional blasting or using a rock breaker machine. This secondary breakage increases costs and can cause environmental hazards such as flyrock and noise.

Therefore, it's essential to minimize the percentage of oversized fragments in every muckpile. This can be achieved by optimizing the design of the drilling, charging, and firing patterns. However, optimization is complicated due to the heterogeneity and anisotropy of rock mass systems, which have varying geotechnical properties like density, hardness, strength, elasticity, and joints. Other variables, such as explosive parameters (density, velocity of detonation), technical parameters (delay interval, primer strength and location), and geometrical parameters (burden, spacing, stemming), also play significant roles (Kulatilake et al., 2010).

Blasts are usually optimized through several field trials, which are time-consuming and expensive. To reduce the number of field trials, it's important to forecast the fragmentation distribution of a blast in each rock mass using the proposed drilling, blasting, and firing patterns. The literature indicates that many models are available for predicting fragmentation, which can be broadly classified as empirical, mechanistic, or artificial intelligence (AI) based models. Users often struggle to choose the model best suited to their needs and conditions. This paper critically reviews each model to help users understand their advantages and disadvantages.

Different factors affect rock fragmentation, which is the breakage of rock material through mechanical excavation or drilling and blasting operations. The outcome of blasting, known as fragmentation, is influenced by numerous factors, some of which are well-known while others are more complex. Key factors affecting rock fragmentation include rock properties such as brittleness, fracture toughness, hardness, compressive strength, and tensile strength. Cutting parameters like cutting depth, attack angle, wedge angle, and cutting velocity also play a role, along with confining stress and joint parameters, including the inclination, orientation, and spacing of joints within the rock. Additionally, the blast-induced wetness of blast holes can impact fragmentation.

The condition of the rock is crucial, as the influence of other factors can vary significantly from one location to another. For example, a change in a parameter in one type of rock can have a significant impact, while the same change in another type of rock may go unnoticed.

Researchers have classified these factors into two main categories: controllable and uncontrollable parameters.

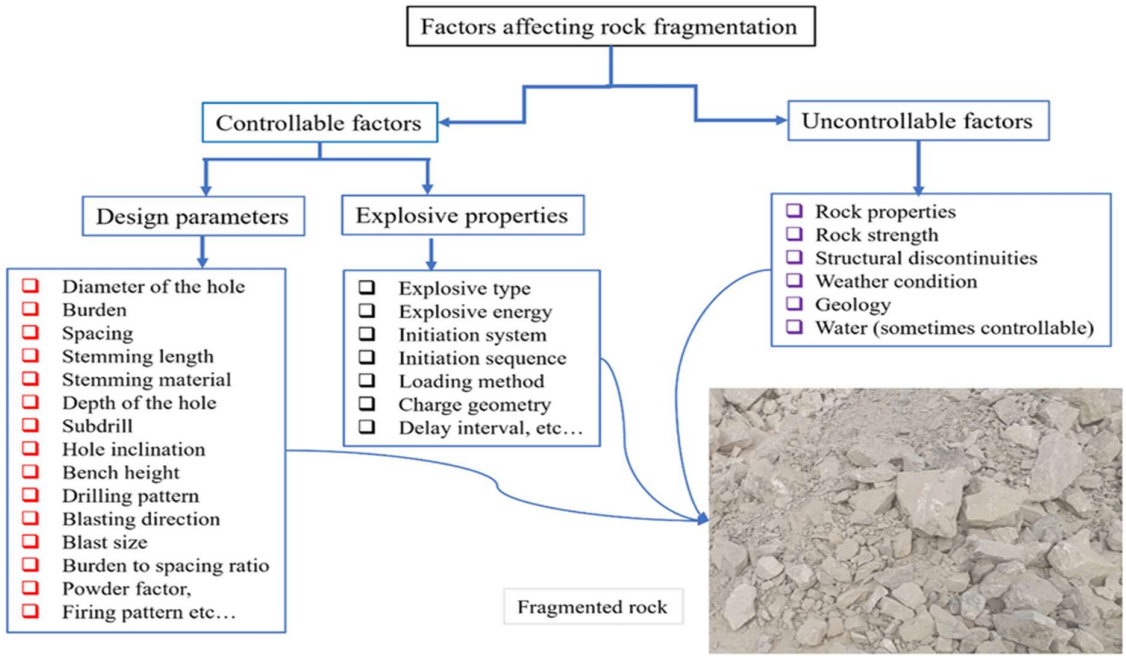

Figure 1 : Factors affecting rock fragmentation.

The estimation of fragmentation distribution becomes important to optimise the drilling and blasting pattern. Literature review has indicated that voluminous work has been done on this aspect. Several models have been suggested by various researchers:

2.1 Modified Kuz-Ram Model:

The Kuz-Ram model is a widely used empirical model for blast fragmentation analysis in mining and quarrying operations. It serves as a predictive tool to estimate the size distribution of fragmented material resulting from explosive blasting. This model has found extensive application in the optimization of blasting parameters to achieve desired fragmentation outcomes, which is crucial for downstream processes such as crushing and grinding (Cunningham, 2005)

The Kuz-Ram model is based on the idea of how energy is distributed within the rock mass during blasting. It assumes that the energy from the explosive is spread among the rock fragments following a power law distribution. This means that different sized fragments absorb different amounts of energy, which affects how they break apart (Cunningham,1987).

The Kuz-Ram model uses several important parameters to describe the blasting process and its impact on rock fragmentation. These parameters include the specific charge (the amount of explosive energy per unit volume of rock), rock mass properties (like density and compressive strength), and blast design elements (such as burden and spacing). By inputting these parameters, along with information about the geology and the desired fragmentation outcomes,

engineers can predict the resulting size distribution of the fragmented material (Cunningham, 1983).

The Kuz-Ram Model, developed in the early 1980s, has been refined over the years, with the 2005 revised equations being the most widely used in the blasting industry. This model uses the Rosin-Rammler distribution and an equation to calculate the uniformity index. A key feature of the Kuz-Ram Model is its ability to predict a complete fragmentation distribution curve without needing any prior fragmentation data. The Modified Kuz-Ram model, (Cunningham, 1987) is presented in Equation 1.

$$x_{50} = Aq^{-0.8}\left(\frac{115}{S_{ANFO}}\right)^{0.633} \qquad \dots Eqn.(1)$$

Where:

x_{50} = 50% passing material size (cm)
A = rock strength factor
q = powder factor (kg explosives/m3 or rock)
Q = weight of explosives in the blasthole (kg)
S_{ANFO} = relative weight strength to ANFO

After calculating the x_{50} value using the modified Kuz-Ram equation and the uniformity index, the entire particle size distribution curve can be determined using the Rosin-Rammler cumulative distribution function. It's important to note that when Cunningham originally proposed the equation, x_{50} was meant to represent the mean particle size. However, he mistakenly used x_{50} to denote the median particle size instead. This error led to the need for a correction to account for the difference between the mean and median values.

The Kuz-Ram model is popular because of its simplicity and ease of use, making it accessible to practitioners without needing extensive computational resources or specialized expertise. However, it is important to remember that the model is based on empirical relationships from observed blast outcomes, so it may not always accurately predict fragmentation, especially with different rock types or blast geometries. Additionally, the model tends to underestimate the amount of fine material produced by blasting, which can cause issues downstream if the model is used to design or adjust the operating parameters of a mineral processing plant. Therefore, the Kuz-Ram model is often used alongside field data and practical experience to refine and validate its predictions, ensuring optimal blasting practices and efficient material processing in mining and quarrying operations.

2.2 Rosin-Rammler Distribution:

The Rosin-Rammler cumulative distribution function was developed in the 1930s for use in coal processing and was later implemented by the blasting industry (Rosin & Rammler, 1933). Equation 4 shows the Rosin-Rammler distribution in terms of current fragmentation distribution functions:

$$P_{RR}(x) = 1 - e^{-\left(\frac{x}{x_c}\right)^n} = 1 - e^{-\ln 2\left(\frac{x}{x_{50}}\right)^n} = 1 - 2^{-\left(\frac{x}{x_{50}}\right)^n} = 1 - 5^{-\left(\frac{x}{x_{80}}\right)^n}$$

…Eqn.2

Where:
$P_{RR}(X)$ = to the percent passing of material size x
x = material size in question
x_C = characteristic size
x_{50} = 50% passing material size
x_{80} = 80% passing material size
n = uniformity index

Using the Rosin-Rammler distribution to predict fragmentation has two main advantages. First, it is relatively simple, requiring only two variables to estimate a cumulative fragmentation curve: the characteristic size (typically the 50% passing size) and the uniformity index (Ouchterlony & Sanchidrian, 2019). Second, it requires significantly less screening to determine the fragmentation distribution.

However, the simplicity of the Rosin-Rammler distribution is also a drawback for predicting fragmentation. According to Worsey (2020), when dealing with material sizes smaller than the 50% passing size, the equation forms a straight line with a slope of n at the 63.2% passing size on a log-log graph. This means the Rosin-Rammler distribution cannot accuratelyestimate sizes below the 50% passing size.

2.3 Kuznetsov-Cunningham-Ouchterlony (KCO) Model:

This model was developed by extending the modified Kuz-Ram model in 2005. The KCO model replaced the Rosin-Rammler function used in the Kuz-Ram model with the Swebrec function (Ouchterlony, 2005). The KCO model uses the Kuznetsov equation (Kuznetsov, 1973) to estimate the mean fragmentation of the blast and the Swebrec function to determine the percentage of material passing a certain sieve size, as shown in Equations 5, 6, and 7.

$$x_{50} = A\left(\frac{V}{Q_e}\right)^{0.8} Q_e^{\frac{1}{6}} \qquad \ldots Eqn.3$$

Where:
x_{50} = 50% passing material size (cm)
A = rock strength factor
V = rock volume broken per blasthole (m3)
Q_e = explosive charge per hole (kg)

One advantage of the KCO model is that it allows users to determine the maximum material size by knowing the burden value and calculating the 50% passing size. However, the KCO model "generalizes the folding parameter b for all blasts and does not include timing" (Worsey, 2020), which can lead to less accurate fragmentation predictions.

2.4 Swebrec Fragmentation Curve:

The Swebrec Fragmentation Curve was developed through a combination of efforts, including European Union-funded projects involving extensive rock and concrete blasts, research by the Swedish Rock Engineering Research, and work by Montanuniversitaet Leoben (Ouchterlony & Sanchidrian, 2019). This work led to a new distribution curve that, unlike the Rosin-Rammler curve, includes a maximum fragmentation size and a curve folding parameter that can be related to the uniformity index of the Kuz-Ram model (Ouchterlony et al., 2006). The equations for the Swebrec function are shown in Equations 6 and 7.

$$P(x) = \frac{1}{\left\{1 + \left[\frac{\ln(\frac{x_{max}}{x})}{\ln(\frac{x_{max}}{x_{50}})}\right]^b\right\}} \qquad \ldots Eqn.\,6$$

where:
$P(x)$ = percent passing size of material size in question, x
x = material size in question (mm)
x_{max} = maximum material size (mm)
x_{50} = 50% passing size (mm)
b = curve folding parameter.

$$b \approx 0.5 * x_{50} * \ln\left(\frac{x_{max}}{x_{50}}\right) \qquad \ldots Eqn.\,7$$

where:
b = curve folding parameter
x_{50} = 50% passing size (mm)
x_{max} = maximum material size (mm)

One advantage of using the Swebrec Fragmentation Curve function is its ability to estimate the maximum material size based on two different percent passing sizes. Additionally, the Swebrec function provides a better estimate of the distribution of fines generated and is more accurate in predicting particle size distribution across a wider range of sizes than the Rosin-Rammler distribution. However, it is important to note that the Swebrec Fragmentation Curve function still struggles to accurately predict particle size distribution at the extremes of the curve, specifically when the percent passing is greater than 80% or less than 20% (Sanchidrian,2015).

2.5 Methodology:

Using available data on blast design and fragmentation, a prediction model was developed through multivariate regression analysis. This model incorporates several parameters: burden, spacing, powder factor, rock factor, blastability index, hole diameter, hole length, subdrill, stemming, charge length, bench height, and the relative weight strength of explosives compared to ANFO.

A random subset of the initial data was used to test the accuracy of the MRA model by comparing its particle size distribution curves with those generated by Artificial Neuron Network (ANN) model. Each model's ability to predict fragmentation outcomes was evaluated using various statistical metrics, including Mean Absolute Error (MAE), Mean Absolute Percentage Error (MAPE), Root Mean Square Error (RMSE), and Relative Root Mean Square Error (RRMSE).

2.5.1 Multivariate Regression Model Development:

To conduct multivariate regression analysis using Microsoft Excel for a project, the following methodology was employed. First, the dataset comprising relevant variables was collected and organized in a spreadsheet. The key parameters included burden, spacing, hole diameter, hole length, top stemming, bench height, charge factor, average explosive per charge, maximum explosive per charge and total explosive. Each row in the dataset represented a distinct blast event, while each column corresponded to one of the aforementioned parameters.

Next, the data was pre-processed to ensure completeness and accuracy, handling any missing values or outliers appropriately. The "Data Analysis" tool in Excel was then used to perform the regression analysis. By navigating to the "Data" tab and selecting "Data Analysis," the "Regression" option was chosen. The dependent variable (target) was set as the fragmentation outcome, while the independent variables (predictors) were the various blast design parameters.

The regression model defined the dependent variables as particle sizes passing at 20%, 50%, and 80%, and independent variables comprises the key parameters included burden, spacing, hole diameter, hole length, top stemming, bench height, charge factor, average explosive per charge, maximum explosive per charge and total explosive. However, through careful analysis and iterative adjustments, the model was refined to include only the seven variables that demonstrated the strongest correlation and predictive power. The final independent variables

included in the MRA model include burden, no of holes, charge factor, top stemming, bench height, maximum explosive per charge and total explosive. This selection of variables led to a more accurate model, likely because it reduced noise and multicollinearity in the dataset, allowing the model to focus on the most significant predictors. By streamlining the model, a better balance between complexity and predictive performance was achieved, enhancing its overall accuracy and interpretability) The analysis was run, yielding a regression output that included coefficients for each parameter, R-squared values, p-values and significance levels. These results were used to construct a predictive model of blast fragmentation.

The model's accuracy was evaluated by comparing its predictions against actual observed outcomes, using statistical metrics such as Mean Absolute Error (MAE), Mean Absolute Percentage Error (MAPE), Root Mean Square Error (RMSE), and Relative Root Mean Square Error (RRMSE).

2.5.2 Artificial Neural Network:

Artificial Neural Networks (ANNs) are mathematical prediction tools that mimic the capabilities of the human brain. This soft computing technique, inspired by the brain's information processing, has seen considerable development and application in fields like engineering geology and rock mechanics. ANNs are effective for tasks involving classification, generalization, characterization, and optimization. They can work with incomplete data, tolerate errors, and gradually converge to form models for complex problems. ANNs are particularly successful in solving semi-structured or non-structured problems.

An ANN consists of densely interconnected adaptive processing units called neurons or nodes. These neurons are arranged in multiple layers, with each layer containing a specific number of neurons based on the problem's complexity. Neurons in one layer connect only to those in the next layer. A multi-layered perceptron neural network includes three types of layers: the input layer (to present data to the network), hidden layers (acting as feature detectors), and the output layer (producing the network's response).

The three main components of an ANN are the learning rule, network architecture, and transfer function. Neurons in each layer are connected to those in the next layer, with each connection carrying a weight. In a back-propagation ANN (BP-ANN), input data propagates from the input layer to hidden neurons through weighted connections. Each input is multiplied by an adjustable weight, and the weighted inputs are summed at each node, combined with a bias value, and passed through a nonlinear transfer function like a sigmoidal function. This process continues layer by layer until the output is generated.

The BP training algorithm iteratively adjusts the weights and biases to minimize system error, a process known as "training" or "learning." The network searches for a set of weights and biases that produce outputs close to the target values. The back-propagation algorithm, popular and readily used, involves two steps:

1. In the forward pass, information from the input layer passes through the network's layers to the output layer, computing the error function, typically the sum of squared errors.
2. In the backward pass, the error propagates backward from the output layer to the input layer, modifying the weights to reduce the error.

This iterative process continues until the ANN achieves high accuracy in its predictions (Haykin,2004).

Neural Network Toolbox (nntool) available in MATLAB. Specifically, we used the Levenberg-Marquardt backpropagation algorithm in combination with the Bayesian regularization algorithm (implemented as the TRAINBR function in MATLAB) for training the neural network. Bayesian regularization was chosen for generalization purposes due to the small dataset. The network's weights and biases were updated using the Levenberg-Marquardt optimization technique.

To prepare the input and target values, we scaled them to a range between -1 and 1 using the following equation:

$$d_{normalized} = 2\left(\frac{d_{original} - d_{min}}{d_{max} - d_{min}}\right) - 1 \qquad \dots Eqn(8)$$

Where, d_{min} and d_{max} are minimum and maximum value of the corresponding parameter, and $d_{normalized}$ is the scaled value.

The dataset was randomly divided into a training set and a testing set, with the training set comprising 75% of the data (28 data points) and the testing set comprising the remaining 25% (10 data points). The data points in each set were mutually exclusive. The network was trained using the training data, which included both the input and target sets. After training, the network's performance was evaluated using the testing data set.

Through several trials and adjustments, we found that the best results were achieved with 10 neurons in the hidden layer. The final network structure included three layers: 7 input neurons, 6 hidden neurons, and 1 output neuron, as shown in figure 1,

CHAPTER-3

ANALYSIS OF DATA

Data was collected for 38 bench blasts at an underground metal mine for use in both model training and model validation. The main data for these parameters for 38 underground bench blasts for model training are shown in Table 1. The measured d20, d50, and d80, data from the 38 bench blasts for model training are shown in Table 2.

Table 1 : Blasting Data for use in Model Training and Validation

Test	No. of Holes	Bench Height (m)	Burden (m)	Top stemming (m)	Q_{max} (Kg)	Q_{total} (Kg)	Charge factor (Kg/m^3)
T1	14	7	2.5	2.4	36	506	0.69
T2	24	5	2.5	2.6	46	617	0.61
T3	15	10	2.5	2.5	38	575	0.51
T4	24	10	2.5	2.7	72	867	0.48
T5	20	10	2.5	2.5	72	728	0.48
T6	24	10	3	3	100	1200	0.56
T7	37	8	2.5	2.5	76	2331	0.63
T8	37	6	2.5	2.5	44	823	0.59
T9	31	8	2.5	2.5	82	1190	0.68
T10	32	6	2.5	2.5	50	775	0.56
T11	24	9	3	3	100	1200	0.62
T12	21	8	2.5	2.5	42	858	0.68
T13	21	7.5	2.5	2.8	42	656	0.57
T14	40	12	2.75	2.5	128	2543	0.65
T15	60	10	2.5	2.5	150	3000	0.67
T16	20	12	2	3	58	1168	0.97
T17	60	5.5	2.5	2.5	54	1500	0.79
T18	24	9.5	3	2.7	96	1200	0.56
T19	18	6	2.5	2.7	26	475	0.58
T20	15	6.5	2.8	3	25	375	0.43
T21	42	4	2	2.4	18	375	0.56
T22	20	11	2.5	2.5	120	1218	0.73
T23	10	10	2.5	3	40	438	0.53
T24	22	4	2	2.5	16	156	0.5
T25	24	6	2.25	2.8	54	650	0.73
T26	58	9	2.5	2.5	78	1500	0.39
T27	47	9	3	3	100	2500	0.62
T28	116	2.5	2.5	2.6	33.4	967	0.51
T29	55	14	3	3	166	4575	0.56
T30	71	11	3	3	122	4350	0.53
T31	28	9	2.8	3	96	1343	0.6
T32	18	6	2.5	2.7	26	475	0.58

T33	36	4	2.75	2.5	38.94	700	0.59
T34	57	10	2.5	2.5	104	2977	0.69
T35	39	8	3	3	85.4	1626	0.43
T36	27	25	3	2.5	306	4125	0.68
T37	60	18	3	2.5	483	7225	0.99
T38	45	24	3	2.5	260	7775	0.6
Q_{max} = Maximum explosive per charge; Q_{total} = Total Explosive							

Table 2:Measured data for d20, d50, and d80 fragment sizes for model training and validation

	Measured Value		
Test	**d_{25} (mm)**	**d_{50} (mm)**	**d_{90} (mm)**
T1	119.8	217	591.5
T2	182.4	313.1	881.6
T3	376.5	604	1538.1
T4	459.6	754.3	1830.1
T5	436.6	748.9	2282.3
T6	261.1	480.7	1065.8
T7	168.6	287.1	800.1
T8	219	373.4	911.4
T9	149.3	264.9	667.2
T10	289.4	442.8	1003.5
T11	176.1	288.5	846.2
T12	141.2	262.9	681.5
T13	249	429.3	999.5
T14	165.7	271.6	723.9
T15	153.8	269.4	699.5
T16	95.01	176.9	435.2
T17	112.9	189.4	443.8
T18	312.3	473.9	1085.8
T19	236.1	403.6	953.9
T20	573.3	991.8	2471.9
T21	325.3	455	1279
T22	112.9	201.4	467.4
T23	335.1	544.8	1453.7
T24	433.3	706	1564.8
T25	114	198.8	488.9
T26	622.4	991.8	2926.1
T27	175.3	287.1	876.9
T28	370.8	682.6	1515.6
T29	260.4	473.9	1416.6
T30	355.9	537.5	1481.6

T31	201.9	330	909.1
T32	247.9	385.9	940.9
T33	202.3	359.1	940.9
T34	117.7	217	501.9
T35	511.8	940.9	2536
T36	125.4	248.8	667.2
T37	88.4	160.5	292.6
T38	201.7	329.9	905

3.1 Analysis of data using Multivariate Regression Model:

Using the data from Table 1 and Table 2, we employed Microsoft Excel's regression functions to determine the regression coefficients for our model equation. We evaluated how well the model fit the data by looking at metrics like R-squared and F-test statistics. Additionally, we used Excel's diagnostic tools to check the assumptions underlying the regression analysis. In interpreting the results, we focused on the significance of the coefficients, indicated by their p-values, and examined the direction and strength of the relationships between the variables.

The coefficients obtained from the multivariate regression analysis were used to formulate the following predictive equations to calculate the particle size passing at 20%, 50%, and 80% (measured in mm).

$$d_{25} = 1040.02 + 0.54 * N + (-2.51) * H + (-213.91) * B + 162.48 * S_L + 1.08 * Q_{max} + (-0.02) * Q_{total} + (-1188.87) * q$$

$$d_{50} = 1524.14 + 1.40 * N + (-1.84) * H + (-314.65) * B + 286.09 * S_L + 1.82 * Q_{max} + (-0.04) * Q_{total} + (-1909.92) * q$$

$$d_{90} = 3992.44 + 3.41 * N + 3.91 * H + (-804.82) * B + 739.88 * S_L + 4.16 * Q_{max} + (-0.09) * Q_{\text{total}} + (-5164.22) * q$$

Where:

N= No. of Holes,
H= Bench Height (m),
B= Burden (m),
S_L= Top Stemming (m),
Q_{max}= Maximum explosive per charge (Kg),
Q_{total}= Total Charge (Kg),
q= Charge Factor (Kg/m^3).

After training the multivariate regression analysis model, we evaluated its performance using ten test cases from the initial dataset. The selected validation data points, shown in Table 3 and Table 4, were chosen to ensure a thorough assessment. This validation process was essential for determining the model's ability to generalize and accurately predict outcomes in mining

scenarios. It provided valuable insights into the robustness and reliability of the MRA model in real-world applications.

Table 3:Blasting Data for use in model validation

Test	No. of Holes	Bench Height (m)	Burden (m)	Top stemming (m)	Q_{max} (Kg)	Q_{total} (Kg)	Charge factor (Kg/m^3)
V1	14	7	2.5	2.4	36	506	0.69
V2	32	6	2.5	2.5	50	775	0.56
V3	21	7.5	2.5	2.8	42	656	0.57
V4	60	5.5	2.5	2.5	54	1500	0.79
V5	20	11	2.5	2.5	120	1218	0.73
V6	47	9	3	3	100	2500	0.62
V7	18	6	2.5	2.7	26	475	0.58
V8	27	25	3	2.5	306	4125	0.68
V9	36	4	2.75	2.5	38.94	700	0.59
V10	24	6	2.25	2.8	54	650	0.73
Q_{max} = Maximum explosive per charge; Q_{total} = Total Explosive							

Table 4:Measured data for d20, d50, and d80 fragment sizes for model validation

	Measured value		
Test	d25 (mm)	d50 (mm)	d90 (mm)
V1	119.8	217	591.5
V2	289.4	442.8	1003.5
V3	249	429.3	999.5
V4	112.9	189.4	443.8
V5	112.9	201.4	467.4
V6	175.3	287.1	876.9
V7	247.9	385.9	940.9
V8	125.4	248.8	667.187
V9	202.3	359.1	940.9
V10	114	198.8	488.9

3.2 Analysis of data using Artificial Neural Network (ANN) Model:

Artificial Neural Networks (ANNs) offer a more complex approach inspired by the human brain's neural networks, making them particularly effective for predictive tasks and pattern

recognition. The data collected for MRA was normalized to a range of -1 to 1 to ensure all input values were comparable. Normalization is done using the following formula:

$$d_{normalized} = 2\left(\frac{d_{original} - d_{min}}{d_{max} - d_{min}}\right) - 1 \qquad \ldots Eqn(9)$$

The ANN used in this study had three layers: an input layer with neurons for each independent variable, a hidden layer with 10 neurons (optimal through trial and error), and an output layer with one neuron representing the predicted mean particle size.

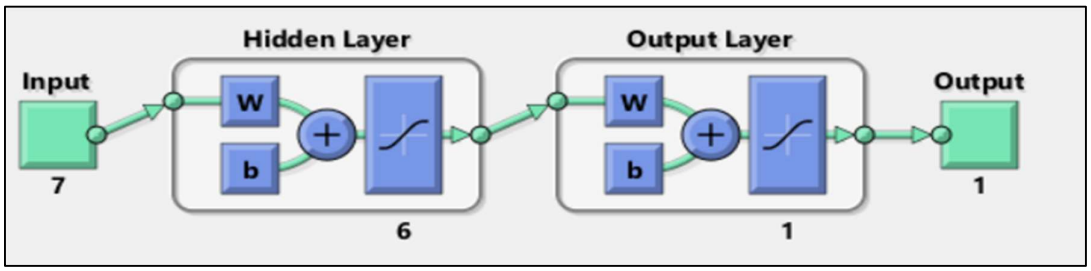

Figure 2:Neural Network showing Input, Hidden and Output layers.

The training set, which constituted 75% of the total data, was used to train the network using the Levenberg-Marquardt backpropagation algorithm combined with Bayesian regularization to optimize weights and biases and prevent overfitting. The remaining 25% of the data was used to test the network. Performance metrics similar to those used for MRA were calculated to evaluate the ANN model's accuracy.

Table 5: Normalized Blasting data for use in model training.

Test	No. of Holes	Bench Height (m)	Burden (m)	Top stemming (m)	Q_{max} (Kg)	Q_{total} (Kg)	Charge factor (Kg/m^3)
T1	-0.74	-0.77	0.00	-0.33	-0.87	-0.88	-0.27
T2	-0.91	-0.30	0.00	-0.67	-0.91	-0.89	-0.60
T3	-0.74	-0.30	0.00	0.00	-0.76	-0.81	-0.70
T4	-0.81	-0.30	0.00	-0.67	-0.76	-0.85	-0.70
T5	-0.74	-0.30	1.00	1.00	-0.64	-0.73	-0.43
T6	-0.49	-0.49	0.00	-0.67	-0.74	-0.43	-0.20
T7	-0.49	-0.67	0.00	-0.67	-0.88	-0.82	-0.33
T8	-0.60	-0.49	0.00	-0.67	-0.72	-0.73	-0.03
T9	-0.74	-0.40	1.00	1.00	-0.64	-0.73	-0.23
T10	-0.79	-0.49	0.00	-0.67	-0.89	-0.82	-0.03
T11	-0.43	-0.12	0.50	-0.67	-0.52	-0.37	-0.13
T12	-0.06	-0.30	0.00	-0.67	-0.43	-0.25	-0.07
T13	-0.81	-0.12	-1.00	1.00	-0.82	-0.73	0.93

T14	-0.74	-0.35	1.00	0.00	-0.66	-0.73	-0.43
T15	-0.85	-0.67	0.00	0.00	-0.96	-0.92	-0.37
T16	-0.91	-0.63	0.60	1.00	-0.96	-0.94	-0.87
T17	-0.40	-0.86	-1.00	-1.00	-0.99	-0.94	-0.43
T18	-1.00	-0.30	0.00	1.00	-0.90	-0.93	-0.53
T19	-0.77	-0.86	-1.00	-0.67	-1.00	-1.00	-0.63
T20	-0.74	-0.67	-0.50	0.33	-0.84	-0.87	0.13
T21	-0.09	-0.40	0.00	-0.67	-0.73	-0.65	-1.00
T22	1.00	-1.00	0.00	-0.33	-0.93	-0.79	-0.60
T23	-0.15	0.07	1.00	1.00	-0.36	0.16	-0.43
T24	0.15	-0.21	1.00	1.00	-0.55	0.10	-0.53
T25	-0.66	-0.40	0.60	1.00	-0.66	-0.69	-0.30
T26	-0.51	-0.86	0.50	-0.67	-0.90	-0.86	-0.33
T27	-0.11	-0.30	0.00	-0.67	-0.62	-0.26	0.00
T28	-0.45	-0.49	1.00	1.00	-0.70	-0.61	-0.87

Table 6: Normalized measured data for d20, d50, and d80 fragment sizes for model training.

Test	d25(mm)	d50(mm)	d90(mm)
T1	-0.65	-0.63	-0.55
T2	0.08	0.07	-0.05
T3	0.39	0.43	0.17
T4	0.30	0.42	0.51
T5	-0.35	-0.23	-0.41
T6	-0.70	-0.70	-0.61
T7	-0.51	-0.49	-0.53
T8	-0.77	-0.75	-0.72
T9	-0.67	-0.69	-0.58
T10	-0.80	-0.75	-0.70
T11	-0.71	-0.73	-0.67
T12	-0.76	-0.74	-0.69
T13	-0.98	-0.96	-0.89
T14	-0.16	-0.25	-0.40
T15	-0.45	-0.42	-0.50
T16	0.82	1.00	0.66
T17	-0.11	-0.29	-0.25
T18	-0.08	-0.08	-0.12
T19	0.29	0.31	-0.03
T20	1.00	-0.91	1.00
T21	0.06	1.00	-0.07
T22	-0.36	0.26	-0.15
T23	0.00	-0.25	-0.10
T24	-0.57	-0.09	-0.53
T25	-0.89	-0.59	-0.84

Test	0.59	-0.52	0.70
T1	-1.00	-0.86	-1.00
T2	-0.58	0.88	-0.53

Table 7: Normalized Blasting data for use in model testing.

Test	No. of Holes	Bench Height (m)	Burden (m)	Top stemming (m)	Q_{max} (Kg)	Q_{total} (Kg)	Charge factor (Kg/m^3)
T1	-0.92	-0.58	0.00	-1.00	-0.91	-0.91	0.00
T2	-0.58	-0.67	0.00	-0.67	-0.85	-0.84	-0.43
T3	-0.79	-0.53	0.00	0.33	-0.89	-0.87	-0.40
T4	-0.06	-0.72	0.00	-0.67	-0.84	-0.65	0.33
T5	-0.81	-0.21	0.00	-0.67	-0.55	-0.72	0.13
T6	-0.30	-0.40	1.00	1.00	-0.64	-0.38	-0.23
T7	-0.85	-0.67	0.00	0.00	-0.96	-0.92	-0.37
T8	-0.68	1.09	1.00	-0.67	0.24	0.04	-0.03
T9	-0.06	0.44	1.00	-0.67	1.00	0.86	1.00
T10	-0.34	1.00	1.00	-0.67	0.04	1.00	-0.30

Table 8:Normalized measured data for d20, d50, and d80 fragment sizes for model testing.

Test	d25(mm)	d50(mm)	d90(mm)
T1	-0.88	-0.86	-0.77
T2	-0.25	-0.32	-0.46
T3	-0.40	-0.35	-0.46
T4	-0.91	-0.93	-0.89
T5	-0.91	-0.90	-0.87
T6	-0.67	-0.70	-0.56
T7	-0.40	-0.46	-0.51
T8	-0.86	-0.79	-0.72
T9	-1.00	-1.00	-1.00
T10	-0.58	-0.59	-0.53

All the data point in the data sets was mutually exclusive. The network is supplied with a set of training data which include training input set and training target set. The network is then tested using testing data set by supplying the testing input set to the developed network. On processing with several trial and errors, it was observed that testing error is very close to the best performing epoch thus indicating that the network developed is not overfitted. The training is stopped when the criteria of maximum epoch was reached.

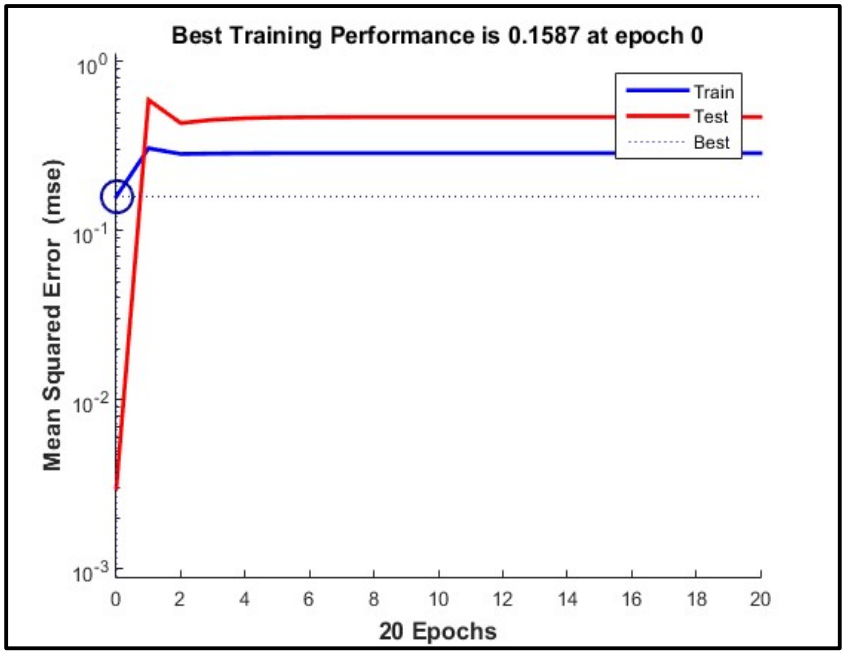

Figure 3: Plot of mean square error v/s epoch for d25 fragment size.

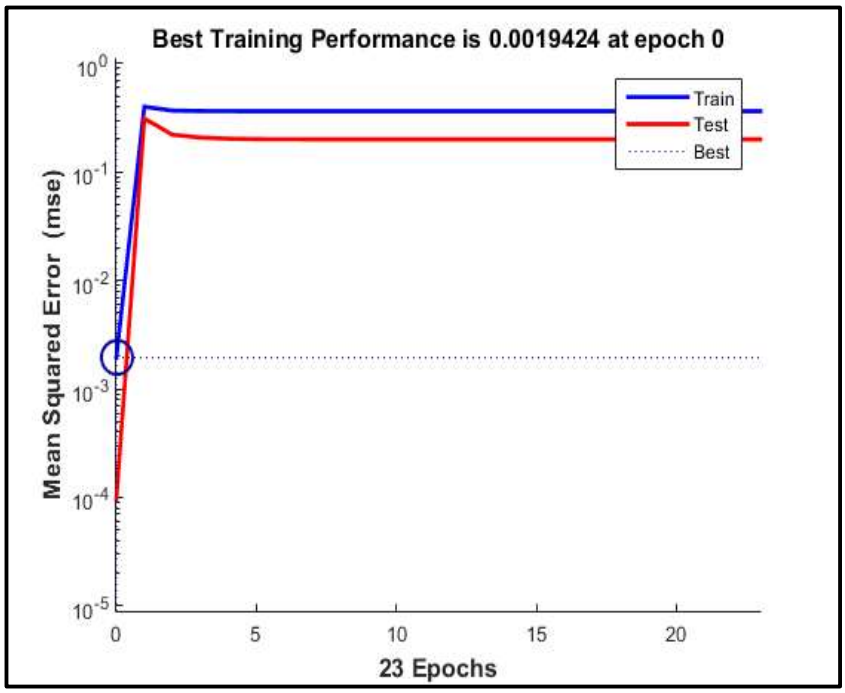

Figure 4:Plot of mean square error v/s epoch for d50 fragment size.

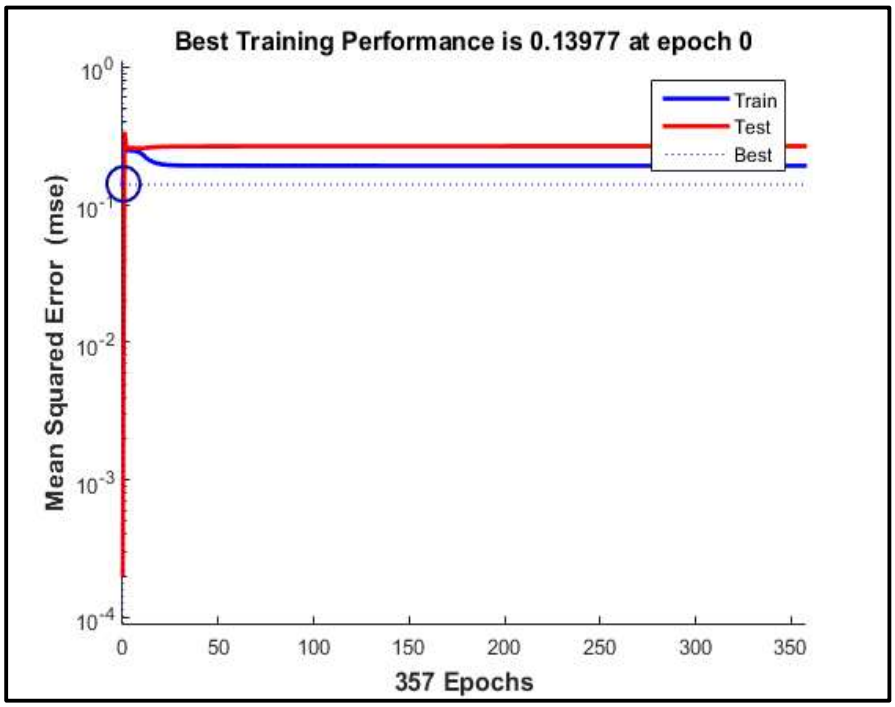

Figure 5: Plot of mean square error v/s epoch for d90 fragment size.

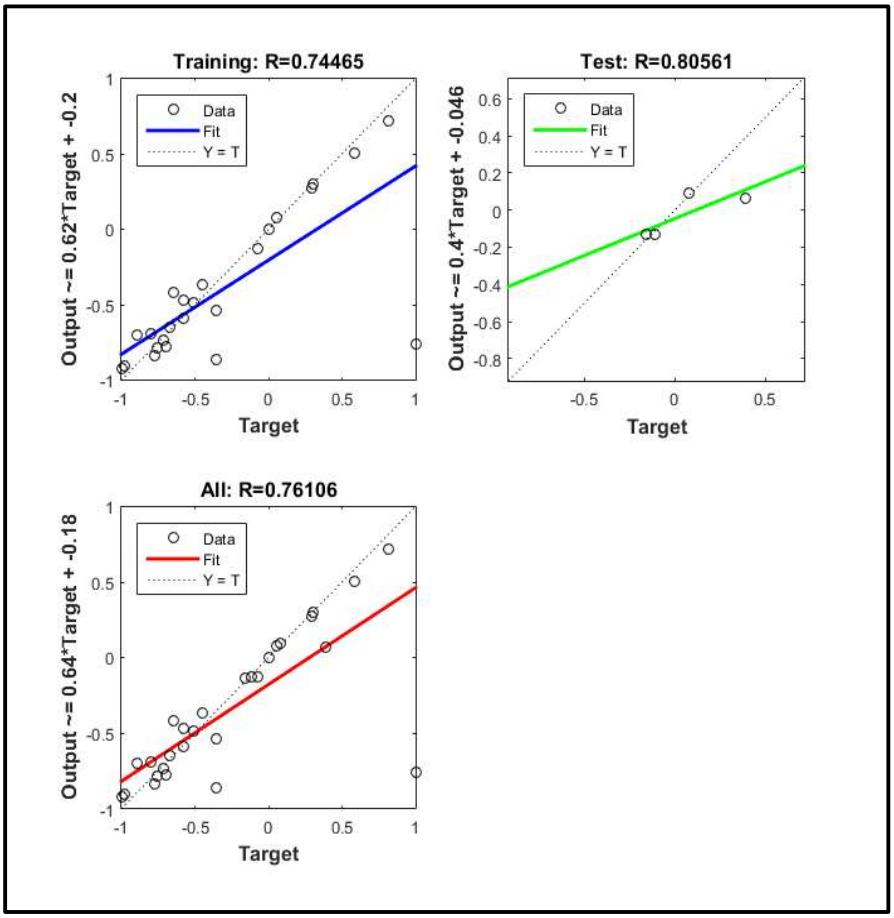

Figure 6:Regression Plot of training and testing data of d25 fragment size.

,

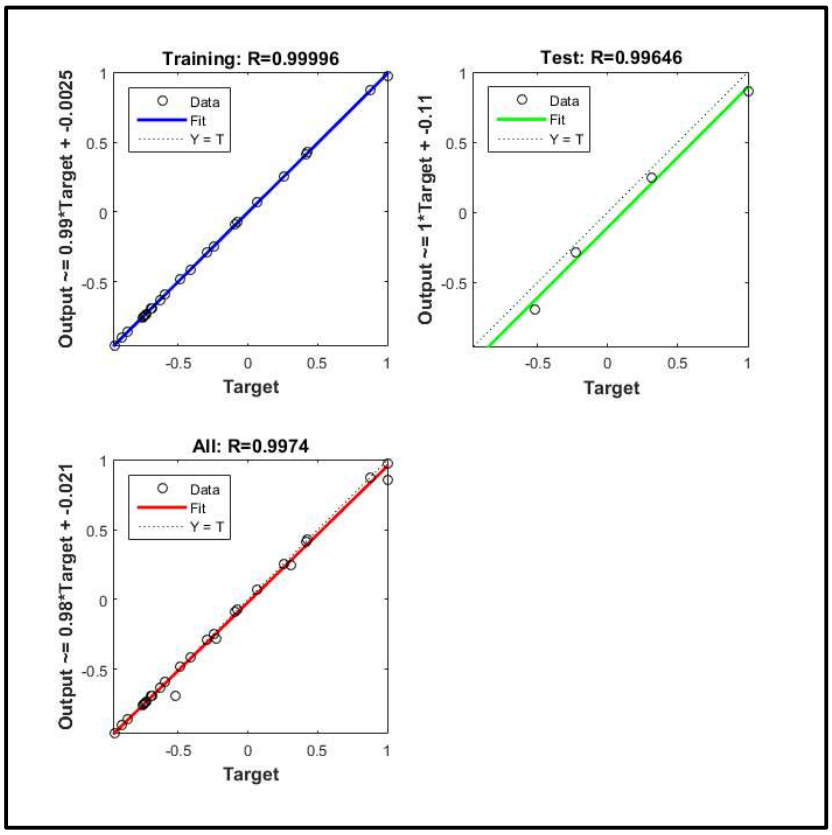

Figure 7:Regression Plot of training and testing data of d50 fragment size.

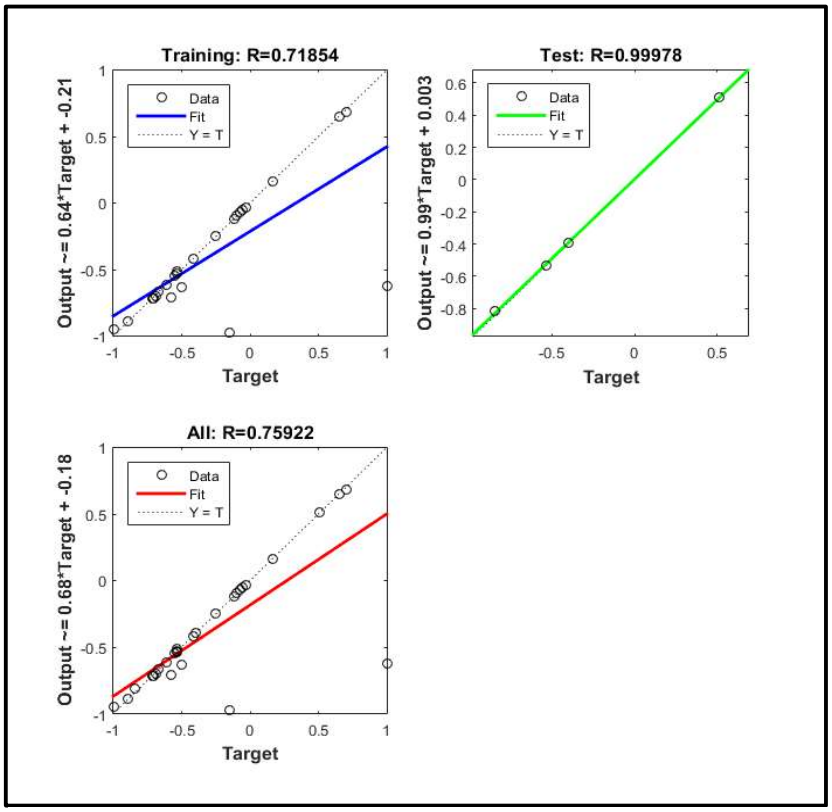

Figure 8: Regression Plot of training and testing data d90 fragment size.

CHAPTER-4

RESULT AND DISCUSSIONS

In evaluating blast fragmentation prediction models, the predicted values of d20, d50, and d80 for the validation data are crucial. These values serve as key benchmarks for assessing each model's accuracy and reliability in predicting blast fragmentation outcomes in mining scenarios. By comparing these predictions with actual fragmentation data, we can gauge the effectiveness of each model in real-world applications. The results of each of the models' predictions for the validation datasets, along with the measured values are shown in Table 9. When comparing the models' ability to accurately predict the d20, d50, and d80 values, the following observations were made.

The multivariate regression analysis (MRA) model demonstrated a higher accuracy in predicting the d20, d50, and d80 values compared to the Artificial Neural Network (ANN) model. For all three metrics, the MRA model's predictions were closer to the measured values, indicating its superior performance in capturing the distribution of blast fragmentation sizes. This suggests that the MRA model is more effective at predicting the key fragmentation metrics, making it a better tool for planning and optimizing blasting operations in mining.

Table 9:Measured and predicted data for d20, d50, and d80 fragment sizes for comparison between models based on model.

	d25(mm)			d50(mm)			d90(mm)		
Test	Measured	MRA	ANN	Measured	MRA	ANN	Measured	MRA	ANN
V1	119.8	93.6	361.6	217	158.3	889.3	591.5	372.1	1828.6
V2	289.4	286.4	346.4	442.8	476.9	891.5	1003.5	1209.0	2709.0
V3	249	307.3	441.0	429.3	515.7	235.6	999.5	1325.1	2843.3
V4	112.9	19.2	331.0	189.4	56.1	179.4	443.8	66.1	2554.5
V5	112.9	132.0	516.6	201.4	235.9	969.9	467.4	561.0	2865.3
V6	175.3	209.4	498.8	287.1	385.5	952.1	876.9	982.3	2807.3
V7	247.9	267.6	342.6	385.9	444.7	629.6	940.9	1133.1	2455.0
V8	125.4	195.9	102.9	248.8	380.4	187.3	667.187	1007.5	411.2
V9	88.4	194.0	94.2	160.5	333.1	183.3	292.6	819.4	303.2
V10	201.7	189.0	119.3	329.9	317.8	192.6	905	754.8	485.5

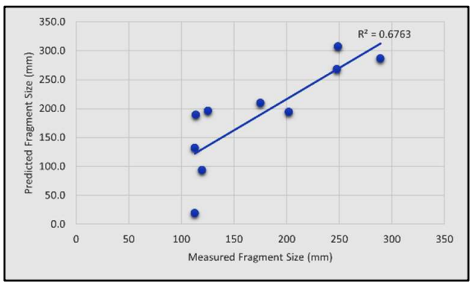

Figure 9: Measured d25 Vs Predicted d25 Fragment size obtain in MVRA.

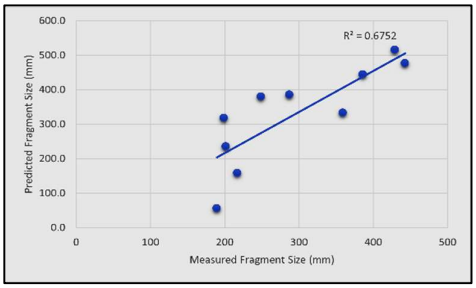

Figure 10: Measured d50 Vs Predicted d50 Fragment size obtain in MVRA.

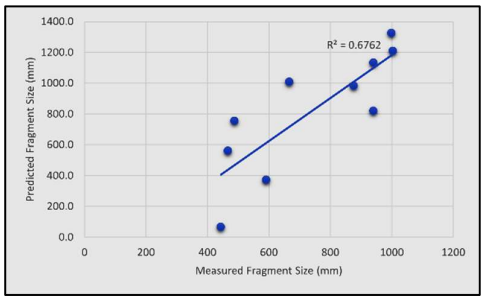

Figure 11: Measured d90 Vs Predicted d90 Fragment size obtain in MVRA.

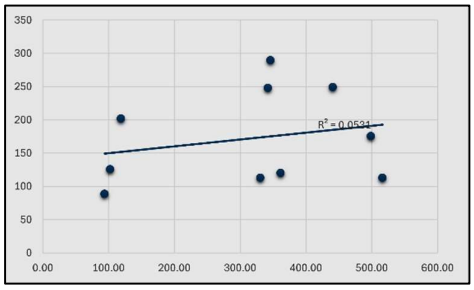

Figure 12: Measured d25 Vs Predicted d25 Fragment size obtain in ANN.

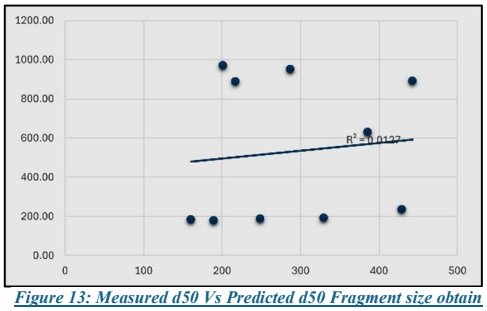

Figure 13: Measured d50 Vs Predicted d50 Fragment size obtain in ANN.

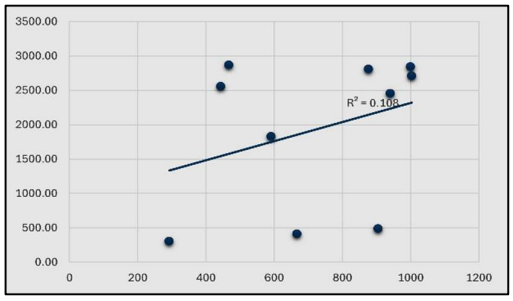

Figure 14: Measured d90 Vs Predicted d90 Fragment size obtain in ANN.

The goal of comparing the predictions from each model was to evaluate the performance of the Multivariate Regression Analysis (MRA) model against established surface blasting models. This comparison aimed to highlight the effectiveness of each model in addressing the unique challenges of blasting operations. The accuracy of each fragmentation model, based on metrics such as Mean Absolute Error (MAE), Mean Absolute Percentage Error (MAPE), Root Mean Square Error (RMSE), and Relative Root Mean Square Error (RRMSE), is detailed in Table 10.

Table 10: Fragmentation model accuracy via statistical metrics values including MAE, MAPE, RMSE, and RRMSE.

	d_{25}		d_{50}		d_{90}	
Stat. Metric	**MVRA**	**ANN**	**MVRA**	**ANN**	**MVRA**	**ANN**
MVA VALUE	40.8	164.2	78.1	29.9	224.7	1342.6
MAPE VALUE (%)	30.0	113.8	31.2	121.8	34.6	121.8
RMSE VALUE	50.5	207.4	87.4	425.0	244.4	1559.0
RRMSE VALUE	0.1	0.2	0.1	0.2	0.1	0.2

To visually compare the performance of the multivariate regression analysis (MRA) model and the Artificial Neural Network (ANN) model using validation datasets, we examined four key metrics: Mean Absolute Error (MAE), Mean Absolute Percentage Error (MAPE), Root Mean Square Error (RMSE), and Relative Root Mean Square Error (RRMSE). When comparing the accuracy of each model's predictive ability, the following observations were made.

The MRA model consistently outperformed the ANN model across all metrics. It had lower MAE, indicating fewer errors in prediction. The MRA model's MAPE was also lower, showing better accuracy in percentage terms. In terms of RMSE, the MRA model again had smaller values, highlighting more precise predictions. Finally, the MRA model's lower RRMSE values demonstrated its superior ability to predict blast fragmentation outcomes with higher reliability. Overall, these results suggest that the MRA model is more accurate and reliable than the ANN model for predicting blast fragmentation in mining operations.

CONCLUSION

This study evaluated predictive models for blast fragmentation, comparing a new multivariate regression analysis model designed specifically for underground blasting scenarios with established models for surface blasting. The evaluation used key metrics such as Mean Absolute Error (MAE), Mean Absolute Percentage Error (MAPE), Root Mean Square Error (RMSE), and Relative Root Mean Square Error (RRMSE) to assess model performance.

The results indicate that the multivariate regression analysis model provides more accurate predictions than the Artificial Neural Network (ANN) model. The multivariate regression consistently showed lower MAE, MAPE, RMSE, and RRMSE values, making it more precise in predicting blast fragmentation outcomes in mining operations. These findings highlight the potential of the multivariate regression model as a valuable tool for optimizing blasting operations. Accurate predictions of blast fragmentation can help mine planners and engineers design more efficient blasting patterns, improve fragmentation control, and ultimately enhance productivity and profitability.

While the study demonstrates the promising performance of the multivariate regression analysis model for underground blast fragmentation prediction, there are opportunities for future research and refinement. Expanding data collection to include a wider range of underground mining environments and conditions could improve the model's robustness and generalizability. Incorporating data from different geological formations, ore types, and operational parameters would provide a more comprehensive understanding of the factors affecting blast fragmentation in underground settings.

Additionally, integrating real-time monitoring data, such as measuring while drilling (MWD), blast vibration measurements, and geotechnical data, could lead to the development of dynamic predictive models. These models could adapt to changing mining conditions, facilitating proactive decision-making and optimization of blasting operations. Exploring machine learning algorithms, such as neural networks or ensemble methods, in conjunction with multivariate regression analysis, could further enhance predictive accuracy by capturing complex nonlinear relationships within the data.

Overall, continued research aimed at refining and advancing predictive models for blast fragmentation is essential to address the evolving challenges and complexities of modern mining operations. Leveraging emerging technologies and methodologies holds the potential to optimize blasting practices, improve fragmentation control, and drive sustainable productivity gains in mining.

ACKNOWLEDGEMENT

I would like to express my sincere gratitude to my guide, Dr. Ranjit Kumar Paswan, for their invaluable guidance and support throughout this research. I also thank CISR-CIMFR for providing the necessary resources.

REFERENCE

1. Aler J., Mouza J.D. and Arnould M. 1996. Measurement of the fragmentation efficiency of rock mass blasting and its mining applications, Int J of Rock Mech and Min Sci and Geo Abstracts. 3: 125- 139.
2. Angesom Gebretsadik, Rahul Kumar, Yewuhalashet Fissha, Yemane Kide, Natsuo Okada, Hajime Ikeda, Arvind Kumar Mishra, Danial Jahed Armaghani, Yoko Ohtomo & Youhei Kawamura (2024). Enhancing rock fragmentation assessment in mine blasting through machine learning algorithms: a practical approach
3. Atkinson, P.M., and Tatnall, A.R. (1997). Introduction neural networks in remote sensing. International Journal of remote sensing, 18(4), 699-709
4. Cunningham, C., 1983. The Kuz-Ram Model for Prediction of Fragmentation from Blasting. Sweden, Lulea University of Technology, pp. 439-453.
5. Cunningham, C., 1987. Fragmentation Estimations and the Kuz-Ram model - Four Years On. 2nd Internatinoal Symposium on Rock Fragmentation by Blasting, pp. 475-487.
6. Cunningham, C., 2005. The Kuz-Ram Fragmentation Model - 20 Years On, Proceedings, Brighton Conference R. Holmberg et al (eds), European Federation of Explosives Engineers, pp. 201-210
7. Dehghani H, Babanouri N, Alimohammadnia F, Kalhori M. Blast-induced rock fragmentation in wet holes. Min Metall Explor. 2020;37(2):743–52.
8. Haykin, S., and Network, N. (2004). A comprehensive foundation. Neural networks, 2(2004), 41
9. Kulatilake P.H.S.W., Hudaverdi T. and Qiong W. 2012. New prediction models for mean particle size in rock blast fragmentation, Geotech and Geological Engineering, 30:665-684.
10. Kulatilake P.H.S.W., Qiong W., Hudaverdi T. and Kuzu C. 2010. Mean particle size prediction in rock blast fragmentation using Neural Networks, Engineering Geology. 114:298-311
11. Kuznetsov, V. M., 1973. The mean diameter of the fragments formed by blasting rock. Journal of Mining Science, Volume 9, pp. 144-148
12. Liu X, Xu M, Qin P. Joints and confining stress influencing on rock fragmentation with double disc cutters in the mixed ground. Tunn Undergr Sp Technol. 2019; 83:461–74.
13. Mulenga S. Evaluation of factors influencing rock fragmentation by blasting using interrelations diagram method. J Phys Sci. 2020;2(1):1–16.
14. Nadolski, S., Klein, B., Elmo, D. & Scoble, M., 2015. Cave-to-Mill: a Mine-to-Mill approach for block cave mines. Mining Technology, pp. 47-55
15. Ouchterlony, F. & Sanchidrian, J., 2019. A Review of Development of Better Prediction Equations for Blast Fragmentation. Journal of Rock Mechanics and Geotechnical Engineering, pp. 1-17.
16. Ouchterlony, F., 2005. The Swebrec Function, Linking Fragmentation by Blasting and Crushing. Mining Technology, Volume 114, pp. 29-44.
17. Ouchterlony, F., Olsson, M., Nyberg, U., Andersson, P., Gustavsson, L. 2006. Constructing the Fragment Size Distribution of a Bench Blast Round, using the New Swebrec Function. Fragblast 8, pp. 332-344.
18. Protodyakonov, M., 1962. Mechanical Properties and Drillability of Rocks. Proceedings, 5th US Symposium on Rock Mechanics, Minneapolis, MN. University of Minnesota, pp. 103-118

19. Rizk, F. H., Saleh, A., Elgaml, A., Elsakaan, A., & Zaki, A. M. (2024). Exploring Predictive Models for Students' Performance in Exams: A Comparative Analysis of Regression Algorithms. Journal of Artificial Intelligence and Metaheuristics (JAIM).

20. Rosin, P. & Rammler, E., 1933. The Laws Governing Fineness of Powdered Coal. Journal of the Institute of Fuel (7), pp. 29-36.
21. Sanchidrian, J., 2015. Ranges of Validity of Some Distribution Functions for Blast-fragmented Rock. Proceedings, 11th International Symposium on Rock Fragmentation by Blasting, pp. 741- 747.
22. Xue Y, Zhou J, Liu C, Shadabfar M, Zhang J. Rock fragmentation induced by a TBM disc-cutter considering the effects of joints: a numerical simulation by DEM. Comput Geotech. 2021; 136:104230.
23. Zhu Z, et al. Contributions of joint structure and free-fall to the fragmentation of rock avalanche: Insights from 3D discrete element analyses. Comput Geotech. 2023; 160:105515–105515.
24. Zou J, Yang W, Han J. Discrete element modeling of the effects of cutting parameters and rock properties on rock fragmentation. IEEE Access. 2020; 8:136393–408.